JCTC Journal of Chemical Theory and Computation

Article

pubs.acs.org/JCTC

High-Accuracy Vibrational Computations for Transition-Metal Complexes Including Anharmonic Corrections: Ferrocene, Ruthenocene, and Osmocene as Test Cases

Camille Latouche,* Federico Palazzetti, Dimitrios Skouteris, and Vincenzo Barone

Scuola Normale Superiore, Piazza dei Cavalieri 7, 56126 Pisa, Italy

Supporting Information

ABSTRACT: Density functional theory calculations of infrared spectra at harmonic and anharmonic levels of theory have been carried out in order to define a reliable yet feasible strategy to perform accurate computations on metal complexes starting from metallocenes. We present different possibilities to compute with unprecedented accuracy either the ligand vibrations or vibrations where the metal atom is involved or even to obtain the entire spectrum without invoking any scaling factor. Anharmonic calculations employing second-order vibrational perturbation theory provide very good results when performed using the B3PW91 hybrid functional associated with an extended basis set and are able to reproduce quantitatively the entire spectrum of ferrocene, including the presence of overtones at ∼1700 cm^{-1}. Furthermore, our results confirm that B3LYP is the best functional to reproduce ligand vibrations, but, unfortunately, it provides unreliable results for vibrations involving the metal atom. Conversely, the PBE0 functional gives accurate results for metal−ligand vibrational frequencies, but it is quite far from the experiment for intraligand ones.

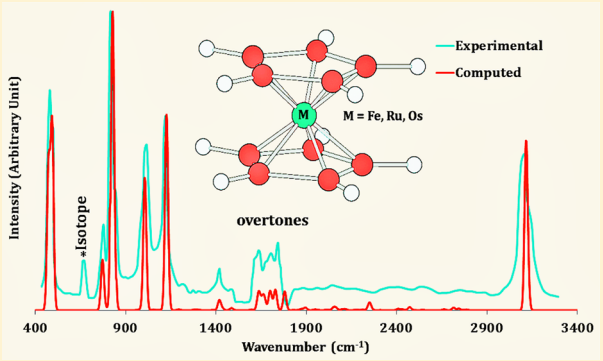

1. INTRODUCTION

Metallocenes are a class of organometallic compounds, formed by a transition metal coordinated to a couple of cyclopentadienyl (Cp = C_5H_5) anions and characterized by a peculiar "sandwich" shape. After the discovery of the prototype ferrocene ($FeCp_2$), many other metallocenes have been analyzed.[1,2] The earliest spectroscopic studies of ferrocene date back to the late 1960s,[3] in the same period when the earliest Raman spectra of ruthenocene ($RuCp_2$) were measured,[4] while the vibrational spectrum of osmocene ($OsCp_2$) was characterized several years later.[5]

Metallocenes and their derivatives are employed as catalysts for olefin polymerization,[6] as glucose biosensors, and even as molecular sensors.[7,8] Moreover, they exhibit antitumoral and nonlinear optical (NLO) properties.[9] Ferrocene, osmocene, and ruthenocene show two nearly isoenergetic conformers: the eclipsed, corresponding to D_{5h} symmetry, and the staggered, corresponding to D_{5d} symmetry. According to both experimental and theoretical studies, the eclipsed conformer is the most stable one for ferrocene in the gas phase,[10−14] as well as for ruthenocene and osmocene. However, in order to characterize the targeted compounds, it is often necessary to perform multifrequency analyses, which are very costly in time and resources. In this respect, methods rooted into density functional theory (DFT) have been instrumental in helping experimental spectroscopy to confirm or disprove experimental hypotheses.[13,14]

Usually harmonic computations are used to this end, possibly improving the absolute accuracy by overall or mode-specific scaling factors.[15−17] More recently, effective approaches have been introduced to allow true anharmonic computations for medium-large size systems at a reasonable cost.[18] In particular, second-order vibrational perturbation theory (VPT2) represents,[18] in our opinion, a very good compromise between accuracy and computational cost, also due to its implementation in general and effective quantum mechanical codes.[19] Furthermore, the recent implementation of infrared (IR) and Raman intensities including both mechanical and electrical anharmonicities is allowing the reproduction of entire spectral shapes and the detection of overtones and combination bands.[18,20] Despite the availability of this technique for several years, so far, comprehensive benchmarks have been performed on electronic transitions[21−25] and IR spectra of organic molecules essentially.[18,26−28]

Therefore, there is a lack of information about the computation of reliable spectroscopic parameters (including anharmonic contributions) for transition-metal complexes and organometallic compounds. As a first step toward filling this gap, we have performed a comprehensive benchmark study at both the harmonic and anharmonic level on metallocene derivatives (M = Fe, Ru, and Os; see Figure 1). Comparison of our VPT2 results with results already available in the literature (experimental and theoretical) shows that only anharmonic computations are able to reproduce the entire IR spectrum,

Received: July 16, 2014

   dx.doi.org/10.1021/ct5006246 | J. Chem. Theory Comput. XXXX, XXX, XXX−XXX

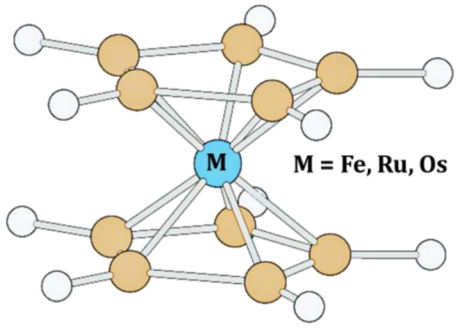

Figure 1. Structure of the studied metallocenes: ferrocene, ruthenocene, and osmocene.

including metal−ligand fundamentals, and explain the origin of some weak peaks in the region of 1600−1800 cm^{-1}.

Even though the number of molecules and combinations of functionals/basis sets is quite small, the results of our study, together with the specific interest in the metallocenes studied, show some general trends that pave the route toward the development of a reliable virtual spectrometer for organometallic systems.

2. COMPUTATIONAL DETAILS

All calculations have been carried out at the DFT level of theory with a locally modified version of the Gaussian suite of programs.[29] On the grounds of previous experience with vibrational spectra of organic molecules,[18] we have selected a classical functional (BP86,[30,31]) employing the generalized gradient approximation (GGA), three widely used hybrid functionals (B3PW91,[31−33] B3LYP,[32,34,35] and PBE0,[36,37]) and a long-range corrected model (CAM-B3LYP, hereafter referenced as CAM[38]). The associated basis sets are the so-called "LANL2DZ",[39−41] including a pseudo-potential on metal atoms and augmented with polarization functions on all atoms (H (*p*; 0.800), C (*d*; 0.587), Fe (*p*; 0.135), Ru (*f*; 1.235), Os (*f*; 0.886)), the so-called "Def2SVP" and "Def2TZVP" basis sets by the Ahlrichs group,[42] a combination of Stuttgart relativistic small core (RSC) pseudo-potential and basis set[43−45] on metal atoms (referred to as SDD) with a 6-311G** basis set on the ligands.[46−49] In the case of ferrocene, we have also performed all-electron computations employing, as suggested by Mohammady et al.,[14] a modified 6-31G* basis set (m6-31G*)[50] on iron and either the 6-31G**[51−54] or the SNSD[55] basis set on other atoms. The SNSD basis set is derived from the 6-31+G** one by adding core−valence and diffuse polarization functions. The different basis sets are summarized in Table 1. After full geometry optimizations, the GVPT2 model has been employed to obtain anharmonic frequencies, taking into proper account all possible resonances, and the DVPT2 model has been used for computing IR intensities including both mechanical and electrical anharmonicities.[18,28] All calculations have been performed in vacuum to be directly comparable to available experimental data.

3. RESULTS AND DISCUSSION

All molecules have been computed in their eclipsed conformation (D_{5h}), which, according to our calculations and to several other theoretical and experimental studies,[10−14,56,57] represents the absolute energy minimum on the potential energy surfaces of those metallocenes in the gas phase. The metallocene structures optimized in the present study are compared to the available experimental data in Tables S1−S3 (see the Supporting Information (SI)). One should notice that, whatever the combination of functional and basis set, the computed geometrical parameters are in good agreement with experimental data and with the CCSD(T) results of a previous study for ferrocene.[10,13] For the case of ferrocene, the Fe−C distances computed at the CAM-B3LYP level are the closest to their experimental counterparts (2.065 and 2.063 Å with basis sets I and II, respectively), whereas both B3PW91 and PBE0 functionals systematically underestimates this distance by ca. 0.02 Å. As is well-known, the computed C−H bond lengths are shorter than the ones observed by X-ray diffraction (XRD). Concerning ruthenocene, the B3PW91 functional associated with the LANL2DZ+pol basis set gives a very good agreement on the Ru−C distances.[11] As for the previous compound, PBE0 underestimates these distances. The computed C−H bond lengths are again shorter than the observed ones. Finally, in agreement with X-ray structures, the computed M−C distances of osmocene and ruthenocene are very close, whereas the C−C distances are slightly longer in osmocene.[57] However, the X-ray structure of osmocene exhibits a large distance range (Os−C range: 2.179−2.200 Å; C−C range: 1.436−1.490 Å), which does not allow, contrary to the cases of ferrocene and rutenocene, a fully quantitative comparison.

3.1. Ligand Vibrations. Let us start from ligand vibrations, which have been unequivocally assigned for all the considered metallocenes. The ligand frequencies of ferrocene computed by different functionals/basi sets are compared to experimental results in Table 2.[58] At the harmonic level, the first two vibrations that correspond to C−H upward and downward motion (γ(C−H)), respectively, are strongly underestimated when BP86 is used, even with a large basis set (II). On the other hand, PBE0 always overestimates the frequencies of both vibrations. On average, the best functionals to reproduce both vibrations are the classical hybrids (B3LYP, B3PW91, and PBE0). Concerning the C−H bending observed at 1012 cm^{-1}, B3LYP at the harmonic level appears particularly close to the experimental value (1018 cm^{-1} with basis set I), while the other functionals tend to overestimate this value. The frequency of the Cp breathing mode at 1112 cm^{-1} is underestimated at the BP86 level and overestimated by the other functionals. The C−C stretching (1416 cm^{-1}) is difficult to reproduce at the harmonic level for all functionals, with an overestimation of 30−60 cm^{-1}, except for BP86, which again underestimates the observed frequency. Whatever the choice of the functional/basis set couple, the C−H stretching frequency (ν(C−H) = 3106 cm^{-1}) is particularly badly reproduced at the harmonic level with an almost-constant overestimation of more than 100 cm^{-1}

Table 1. List of Basis Sets Used in the Present Benchmark (M = Fe, Ru, Os)

	Basis Set					
atom	I	II	III	IV	V	VI
C, H	LANL2DZ+pol	Def2TZVP	6-311G**	6-31G**	SNSD	Def2SVP
M	LANL2DZ+pol	Def2TZVP	SDD	m6-31G*	m6-31G*	Def2SVP

dx.doi.org/10.1021/ct5006246 | J. Chem. Theory Comput. XXXX, XXX, XXX−XXX

Table 2. Comparison of the Experimental Ligand Vibrational Frequencies in Ferrocene with Their Computed Harmonic and Anharmonic (Shown in Parentheses) Counterparts

	Vibrational Frequency (cm^{-1})																					
	I				II				III			IV			V							
Exp[58]	BP86	B3LYP	B3PW91	PBE0	CAM	BP86	B3LYP	B3PW91	PBE0	CAM	B3LYP	B3PW91	PBE0	B3LYP	B3PW91	PBE0	B3LYP	B3PW91	PBE0	B3LYP	B3PW91	PBE0
816	790 (780)	818 (803)	825 (815)	830 (819)	835 (822)	798 (789)	827 (817)	832 (824)	836 (828)	843 (833)	831 (818)	837 (826)	841 (831)	844 (827)	848 (833)	852 (838)	822 (824)	829 (827)	833 (832)			
840	799 (795)	833 (820)	838 (831)	843 (835)	856 (843)	822 (806)	853 (835)	858 (842)	861 (846)	874 (857)	852 (831)	858 (840)	861 (845)	869 (845)	873 (852)	876 (857)	853 (832)	856 (840)	860 (843)			
1012	985 (964)	1018 (998)	1023 (1004)	1029 (1010)	1032 (1013)	992 (972)	1025 (1004)	1028 (1008)	1033 (1014)	1039 (1020)	1024 (1003)	1027 (1008)	1033 (1014)	1031 (1010)	1035 (1013)	1041 (1020)	1022 (1002)	1025 (1006)	1030 (1011)			
1112	1097 (1073)	1130 (1113)	1141 (1124)	1152 (1135)	1155 (1139)	1102 (1084)	1135 (1118)	1144 (1128)	1154 (1138)	1159 (1143)	1134 (1117)	1144 (1127)	1155 (1138)	1138 (1119)	1147 (1128)	1158 (1139)	1132 (1114)	1141 (1126)	1152 (1135)			
1416	1390 (1359)	1447 (1416)	1451 (1421)	1461 (1431)	1472 (1446)	1397 (1363)	1455 (1421)	1455 (1423)	1463 (1432)	1480 (1450)	1452 (1417)	1453 (1421)	1462 (1432)	1464 (1433)	1464 (1429)	1473 (1439)	1450 (1415)	1450 (1418)	1459 (1427)			
3106	3169 (3028)	3250 (3120)	3267 (3140)	3282 (3154)	3275 (3152)	3157 (3021)	3240 (3108)	3247 (3117)	3259 (3131)	3263 (3137)	3234 (3103)	3244 (3116)	3258 (3132)	3253 (3120)	3266 (3133)	3281 (3151)	3234 (3103)	3244 (3115)	3258 (3130)			

by the hybrid functionals. Thanks to fortuitous error compensation, BP86 reproduces this vibrational frequency at the harmonic level better than the other functionals.

Upon the addition of anharmonic corrections, computed and experimental values come in much better agreement. One can notice that, using PBE0, the second vibration is nicely reproduced in almost every case (I, II, III, V) when the anharmonic corrections are included in the computations and the disagreement becomes less than 6 cm^{-1}, with respect to experimental data. The CAM-B3LYP functional strongly overestimates both vibrations at the harmonic level, but the agreement becomes much better upon addition of anharmonic contributions, although the computed value remains quite far from the experimental result. The best agreement for those two vibrations is obtained by anharmonic computations with a hybrid functional. The C−H bending frequencies obtained at the PBE0 level after anharmonic corrections are the best computed ones, and show a remarkable agreement with their experimental counterparts. Furthermore, in almost every case, B3LYP and B3PW91 functionals slightly underestimate the observed vibration while BP86 dramatically underestimates the experimental value. The Cp breathing frequencies computed by the B3LYP functional with anharmonic corrections are in remarkable agreement with experiment for all the considered basis sets. B3PW91, PBE0, and CAM-B3LYP functionals overestimate this vibrational frequency by respectively ca. 15, 25, and 29 cm^{-1}, while BP86 once again underestimates it. As mentioned above, the C−C stretching is badly reproduced at the harmonic level. However, anharmonic B3LYP and B3PW91 results are in remarkable agreement with the experiment, with the error being within 5 cm^{-1} for basis sets I, II, III, and V. Concerning the C−H stretching, when the anharmonic corrections are taken into account, the GGA functional badly reproduces the vibrational frequency, while hybrid functionals provide quite accurate values, especially when employing Becke's exchange.

For all Cp vibrations, it turns out that the BP86 and CAM-B3LYP functionals give unsatisfactory results. BP86 underestimates all observed frequencies except C−H stretchings at the harmonic level, probably again due to error compensation. Moreover, when anharmonic calculations are performed, the discrepancy with experiment actually increases. Vibrations computed with CAM-B3LYP lead to the opposite trend with a constant overestimation of the observed bands, especially for the higher frequencies. The agreement is slightly better when PBE0 is used but the C−H stretching vibration is still strongly overestimated even with anharmonic corrections. A remarkable agreement between computed anharmonic frequencies and their experimental counterparts for the Cp vibrations is obtained when using Becke's exchange[32] especially combined with LYP correlation:[35] as a matter of fact, B3LYP coupled with II and V basis sets, gives quantitative agreement (in the range of ±10 cm^{-1}) with experimental data.[14,59]

Comparison of computed frequencies with the available experimental data points out the non-negligible role of anharmonic corrections (see Figure S1 in the SI). Once again, for the BP86 functional a better agreement is obtained at the harmonic level, because of simultaneous neglect of anharmonic red shifts and intrinsic underestimation of vibrational frequencies. The other functionals have a mean absolute error (MAE) in the range of 30−60 cm^{-1} at the harmonic level for those vibrations, but inclusion of anharmonic effects dramatically decreases the error.

dx.doi.org/10.1021/ct5006246 | J. Chem. Theory Comput. XXXX, XXX, XXX−XXX

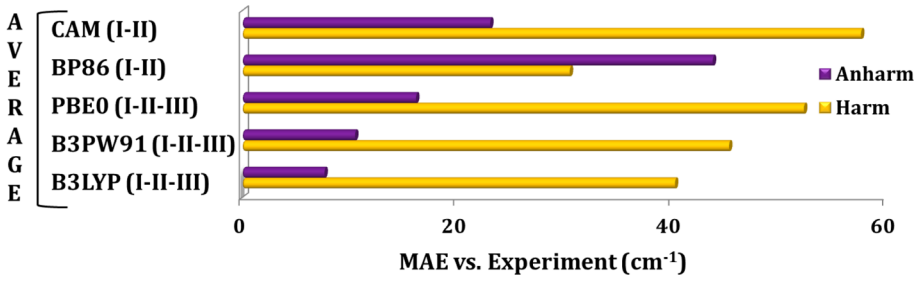

Figure 2. Average errors on the ligand frequencies of the studied metallocenes by different functionals with the basis sets indicated in parentheses. Note that, for BP86 and CAM-B3LYP, the third basis set has not been included.

For instance, harmonic PBE0 frequencies overestimate the experimental values by more than 40 cm^{-1}, but the error is more than halved when anharmonic effects are taken into account, the effect being particularly significant, as expected, for CH stretches. The CAM-B3LYP functional cannot be recommended for computing ligand vibrations in view of its significantly larger error at both harmonic and anharmonic levels. Finally, anharmonic computations with the B3PW91 functional, associated with basis sets II and III lead to an absolute average error below 10 cm^{-1}, which is further reduced up to ca. 5 cm^{-1} by the B3LYP functional with basis sets II or IV. These last results extend the confidence in this methodology from organic molecules to ligand frequencies in metal complexes.

Since the results for the other two metallocenes follow trends similar to those of ferrocene, the corresponding data are given in the SI (Tables S3 and S4). Also, for ruthenocene (Table S3 in the SI) the harmonic results generally overestimate the experimental values for all the bands, the overestimation increasing with the frequency. Upon inclusion of anharmonic effects, the peaks fall into place and are directly comparable to the experimental results. An exception to this trend is represented by the BP86 functional, whose harmonic results tend to fall closer to experiment than anharmonic ones (evidently because of error cancellation).

The two lowest experimental peaks of ruthenocene have been assigned to the γ(C−H) and asymmetric γ(C−H) motions, respectively. Both these frequencies are systematically underestimated by the BP86 functional, whereas the situation is reversed for the CAM-B3LYP functional. An exception to this trend is offered by the LANL2DZ basis set, which leads to the right value at the anharmonic level for the lower-frequency band and actually red-shifts the position (at the harmonic level) of the higher-frequency one (a similar trend can also be observed in the case of osmocene). The other three functionals (B3LYP, B3PW91, and PBE0) generally perform much better in predicting the positions of these two bands, as can also be seen in Figure S2 in the SI. The frequency of the third band is severely underestimated by the BP86 functional (the predicted frequency is systematically off by ∼40 cm^{-1} in all cases). All other functionals approximate it much better, with CAM-B3LYP performing best in this respect. The fourth band (corresponding to the Cp breathing motion) shows a different trend, with a systematic underestimation by the BP86 functional (by ∼30 cm^{-1}) and a corresponding, albeit smaller, overestimation (∼15−20 cm^{-1}) by both PBE0 and CAM-B3LYP functionals. On the other hand, B3LYP and B3PW91 functionals provide a remarkably accurate frequency for this band, irrespective of the employed basis sets. The same picture is seen for the last two observed bands, with B3LYP and B3PW91 providing the best results, BP86 underestimating systematically both frequencies and PBE0 like CAM-B3LYP overshooting them.

We start the discussion on osmocene from the first two observed vibrations.[60] For the latter one, two peaks have been recorded and the one at 852 cm^{-1} has been chosen due to the similarity between observed and computed intensity (see Table S4 in the SI). Once again, BP86 underestimates the frequencies of both vibrations while CAM-B3LYP has the opposite behavior. Except with LANL2DZ+pol basis set, the hybrid functionals overestimate by 10−20 cm^{-1} those two vibrations at the harmonic level. The Cp breathing frequency is ∼15 cm^{-1} lower than the corresponding ones for ruthenocene or ferrocene. One should notice that the use of BP86/II leads to an acceptable reproduction of this vibration. The vibrations at 1395 and 3080 cm^{-1} for osmocene correspond to the ones observed ca. 20 cm^{-1} higher for ruthenocene and ferrocene. Concerning Cp breathing, the best reproduction at the harmonic level is obtained with the BP86 functional, probably due to some error cancellations.

Upon addition of anharmonic terms, the three hybrid functionals provide remarkably accurate results when coupled to extended basis sets (II, III), with, for instance, a B3LYP/II error less than 2 cm^{-1}. The same trend is obtained for the third vibration; however, in this case, the PBE0 functional leads a systematic overestimation of ca. 10 cm^{-1}, with respect to experiment. Once again, the B3LYP and B3PW91 functionals provide the best reproduction of experimental vibrational frequencies, especially with an extended basis set (II). The frequency decrease associated with the Cp breathing mode is reproduced at the B3LYP level when including anharmonic corrections, but this is not the case for the other functionals. As a matter of fact, the B3PW91 value is ca. 1110 cm^{-1} and the corresponding PBE0 (and CAM-B3LYP) result often reaches 1120 cm^{-1}, which is rather far from the recorded frequency. The decreases of the last two frequencies are only barely reproduced by our computations where the most accurate results are obtained at the B3LYP level. The origin of this disagreement can be traced back to different reasons including possible limitations of the representation of relativistic effects by the core potential even for vibrations associated with ligands. However, it is also possible that experimental spectra (or their interpretation) have some problems.

In any case, inclusion of anharmonic effects always improves the agreement between computations and experiment, especially at high frequencies (see Figure S3 in the SI). The only exception is represented by the BP86 functional, whose harmonic results are quite good, because of fortuitous error compensation, and are actually worsened by the addition of anharmonic contributions. At the harmonic level, PBE0 and

dx.doi.org/10.1021/ct5006246 | J. Chem. Theory Comput. XXXX, XXX, XXX−XXX

CAM-B3LYP functionals provide similar results, which are very far from the observed ones. However, upon addition of anharmonic corrections, PBE0 provides better results than CAM-B3LYP, with an absolute average error of ~19 cm^{-1} with basis set II, whereas CAM-B3LYP remains at 30 cm^{-1} when associated with basis set II. Becke's exchange functional provides the best agreement with experimental results especially with a sufficiently extended basis set. One should remark that the B3LYP and B3PW91 results with basis sets II and III are in good agreement with experiment for all infrared frequencies. In the case of B3LYP/II, the average error at the harmonic level is 47 cm^{-1}, but inclusion of anharmonic contributions leads to a much better agreement (9 cm^{-1}).

The performances of the different functionals for ligand vibrations are summarized in Figure 2. It is apparent that the average absolute error on all metallocenes is very low for the B3LYP functional and still acceptable for B3PW91 and (possibly) PBE0. On the other hand, CAM-B3LYP and, especially, BP86 give average errors well above 20 cm^{-1}.

3.2. Metal−Ligand Vibrations and Full IR Spectrum of Ferrocene. The experimental M-Cp vibrational frequencies of ferrocene are compared in Table 3 to those computed at both the harmonic and anharmonic levels of theory.

The first Fe-Cp vibration recorded at 170 cm^{-1} corresponds to the bending between both ligands and the metal (δ CpFeCp). For this vibration, the computed data at the harmonic and anharmonic levels are in good agreement with experiment (as already reported),[59] especially with the B3PW91 and PBE0 functionals. However, one should notice that BP86 and B3LYP functionals slightly underestimate the frequency of this vibration. The band at 480 cm^{-1} corresponding to the Fe-Cp stretching is significantly red-shifted by all the computations at the harmonic level (irrespective of the employed basis set), except in the case of B3PW91 and PBE0 functionals. The last vibration involving the metal atom is the ring tilt at 490 cm^{-1}. Once again, the BP86, B3LYP, and CAM-B3LYP functionals underestimate the frequency associated with this vibration, whereas the B3PW91 and PBE0 values are quite close to the experiment.

Upon anharmonic corrections, BP86, B3LYP, and CAM-B3LYP functionals clearly underestimate the experimental value of Fe-Cp stretching (457, 435, and 456 cm^{-1} for BP86, B3LYP, and CAM-B3LYP with basis set II, respectively). B3PW91 and PBE0 are more successful in reproducing the experimental value when basis sets IV and V are used (476 and 482 cm^{-1} (B3PW91); 473 and 479 cm^{-1} (PBE0) for basis sets IV and V, respectively). The agreement is remarkable concerning the ring tilt (491−499 cm^{-1} vs 490 cm^{-1} experimentally). BP86 results systematically underestimate the frequencies for vibrations involving the metal atom. Surprisingly, B3LYP gives very bad results concerning the M-Cp vibrations with a strong underestimation of the frequencies, even with an extended basis set (II). CAM-B3LYP did not give good results for ligand vibrations and the same discrepancy is obtained concerning the M-Cp vibrations. In summary, it seems that the best way to reproduce the experimental results for vibrations involving the metal atom involves use of PBE0 or B3PW91 functionals associated with basis set V and including anharmonic contributions.

In Figure 3, we compare the absolute average errors between anharmonic computations and experiment for all vibrations of ferrocene. One should notice that BP86 is definitely unable to reproduce all the vibrational frequencies. The CAM-B3LYP functional, which includes some long-range corrections, is also far from the most accurate functional. Furthermore, Figure 3

Table 3. Comparison of Experimental Fe-Cp Vibrational Frequencies of Ferrocene with Their Computed Harmonic and Anharmonic (Shown in Parentheses) Counterparts

	Vibrational Frequencies (cm^{-1})																							
	I				II						III			IV			V							
Exp[58]	BP86	B3LYP	B3PW91	PBE0	CAM	BP86	B3LYP	B3PW91	PBE0	CAM	B3LYP	B3PW91	PBE0	B3LYP	B3PW91	PB0	B3LYP	B3PW91	PBE0					
170	166 (161)	165 (162)	172 (170)	172 (165)	170 (165)	164 (160)	163 (158)	169 (167)	169 (166)	167 (162)	164 (158)	172 (170)	172 (169)	163 (159)	169 (166)	169 (165)	164 (156)	170 (165)	169 (164)					
480	460 (445)	440 (429)	467 (455)	476 (462)	462 (450)	470 (457)	447 (435)	473 (461)	479 (468)	467 (456)	452 (438)	477 (464)	484 (471)	467 (454)	490 (476)	496 (482)	462 (450)	486 (473)	492 (479)					
496	475 (463)	457 (448)	485 (475)	495 (485)	478 (469)	490 (482)	472 (463)	500 (491)	508 (499)	493 (484)	465 (456)	494 (485)	502 (493)	487 (477)	513 (502)	521 (510)	476 (467)	502 (493)	509 (499)					

dx.doi.org/10.1021/ct5006246 | J. Chem. Theory Comput. XXXX, XXX, XXX−XXX

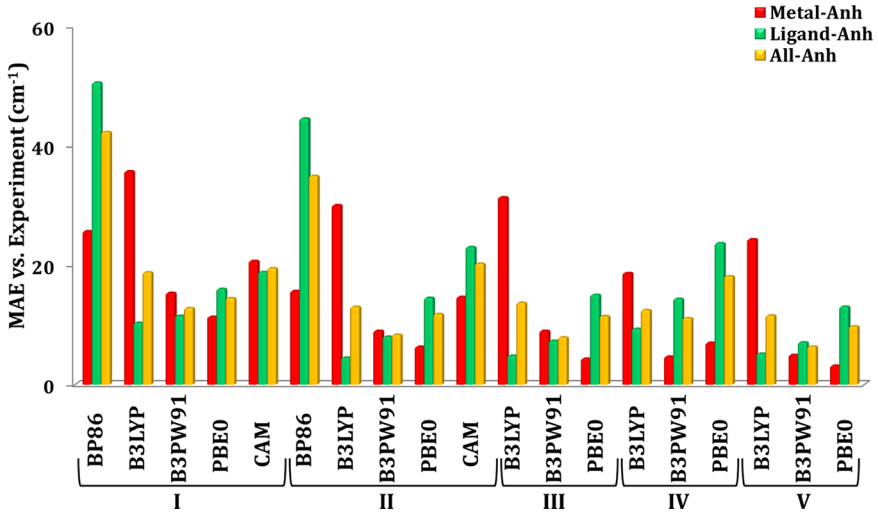

Figure 3. Absolute averaged errors on all vibrations between anharmonic computations and experiment.

Table 4. Anharmonic Corrections for Ferrocene with B3LYP and PBE0 (Basis Sets I–V)

Anharmonic Corrections (cm^{-1})									
B3LYP					PBE0				
I	II	III	IV	V	I	II	III	IV	V
3	5	6	4	8	7	3	3	4	5
11	12	14	13	12	14	11	13	14	13
9	9	9	10	9	10	9	9	11	10
15	10	13	17	−1	11	8	10	14	0
13	18	21	24	20	8	15	16	19	17
20	21	21	21	20	19	19	19	21	19
17	17	17	19	18	17	16	17	19	17
31	34	35	31	35	30	31	30	34	32
130	132	131	133	131	128	128	126	130	128

shows clearly that B3LYP is the best functional to compute ligand vibrations, but leads to quite large errors when the metal atom is involved. On the other hand, PBE0 is far from being the most accurate functional for the ligand vibrations, but it becomes the best one when one wants to focus on the Fe-Cp vibrations with an average error of <5 cm^{-1}. Finally, the best functional to address both ligand and metal–ligand vibrations at the same time is B3PW91 with a total average error <10 cm^{-1} with the basis sets II (8 cm^{-1}), III (8 cm^{-1}), and V (6 cm^{-1}). This latter result suggests that the PW91 correlation is better suited to address vibrations involving transition-metal atoms than its LYP counterpart.

The anharmonic corrections on all vibrations for ferrocene with two functionals (B3LYP and PBE0) and basis sets I–V are given in Table 4. One should remark that the higher is the vibrational frequency, the largest becomes the anharmonic correction (from 3 to 130 cm^{-1}). Furthermore, the choice of the basis set has only a slight impact on the vibrational frequencies (around ±5 cm^{-1}), except in the case of basis set V for the vibration at ∼820 cm^{-1}, where the correction is almost vanishing, whereas for other basis sets, the correction is ∼14 and ∼11 cm^{-1} for B3LYP and PBE0, respectively. This latter result suggests that the critical point to compute with accuracy vibrational energies is to obtain good data at the harmonic level because the anharmonic corrections are very close for different basis sets.

In Figure 4, the experimental IR spectrum of ferrocene is compared to our simulations at the harmonic level (shown in red), as well as the anharmonic level (shown in green). We have chosen to present the spectrum resulting from the use of the B3PW91 functional for purposes of comparison, as this functional has provided the most consistent results for different types of vibrations. Before starting the discussion, let us recall that both mechanical and electric anharmonicities have been taken into account for intensities.

Comparison of harmonic and anharmonic results shows that anharmonicity displaces most peaks nearly exactly on top of their experimental counterparts. In essentially all cases, anharmonic contributions red-shift the corresponding harmonic peak and this can be understood as a dominant second-order correction of the $v' = 1$ level, because of mixing with the $v' = 2$ level caused by the cubic anharmonic terms. This is borne out by the approximate proportionality of the anharmonic correction to the square of the frequency of the band, as would be expected from a cubic correction of the second order (assuming the third derivatives of the potential to be of similar orders of magnitude). As a result, the low frequency bands (corresponding to motion of the iron atom) hardly show any anharmonic correction. As one moves to bending and ring-tilting motions, the anharmonic corrections become more substantial and reach a maximum for bands involving a C–H stretch.

The symmetry species of the IR active bands in the D_{5h} point group are A_2'' (parallel bands) and E_1' (perpendicular bands). The bands at ∼850, 1020, 1400, and 3240 cm^{-1} are all perpendicular, while the ones at ∼820 and 1120 cm^{-1} and the right shoulder at ∼3250 cm^{-1} are parallel. The strongest intensities are predicted for the parallel bands at ∼820 and

dx.doi.org/10.1021/ct5006246 | J. Chem. Theory Comput. XXXX, XXX, XXX–XXX

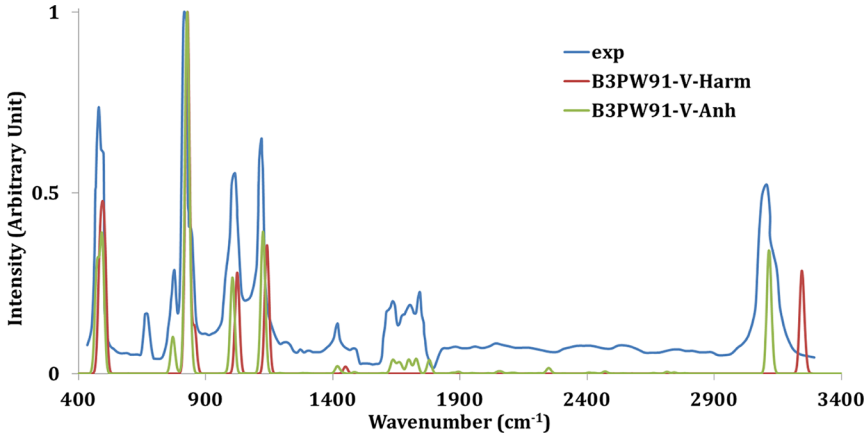

Figure 4. Comparison between experimental (blue) and computed at the harmonic (red) and the anharmonic (green) levels of theory of IR spectra of ferrocene under vacuum. "Exp" data taken from ref 58; "Theo" is B3PW91/V.

1120 cm^{-1} with the perpendicular ones at 450, 1020, and 3240 cm^{-1}. However, one should bear in mind that perpendicular bands are doubly degenerate and thus, transition dipole moments being equal, are favored in intensity by a factor of 2. Moreover, perpendicular bands contain strong, localized Q branches as opposed to parallel ones and this is also a factor that renders the former ones more visible. This pattern is confirmed by the experimental spectrum. One reasonably strong peak at ~630 cm^{-1} is not found in our calculations. Its position, with respect to the strong parallel peak near 820 cm^{-1} (displaced by a factor of ~1.3), suggests very strongly that its origin is the C−D bending motion of monodeuterated ferrocene. We would also like to draw attention to the broad band observed at ~1700 cm^{-1}. It does not correspond to any fundamental band of ferrocene, but it is predicted in our calculations as a set of overtones. Again, the strong anharmonicity mixing between the $v' = 1$ and $v' = 2$ states renders these bands visible in the IR region.

Finally, Figure 4 also exhibits a remarkable agreement concerning the shape and the intensities of the bands. The intense peak at ~850 cm^{-1} and the smaller one at 820 cm^{-1} are well-reproduced with anharmonic corrections, whereas this is not the case at the harmonic level. Furthermore, both distinct peaks at ~500 cm^{-1} are not present within a typical harmonic calculation but the shoulder appears when anharmonic effects are taken into account. This good trend between computed and experiment concerning intensities is also present for further peaks such as the overtones and the final peak at ~3000 cm^{-1}.

The last part of this discussion is devoted to the computational time. The combination of "optimization + harmonic" calculations is always quite inexpensive, but inclusion of anharmonic terms causes substantial lengthening of the computational time (roughly 1−2 orders of magnitude, with respect to the corresponding harmonic frequencies). A possible way of circumventing this bottleneck is offered by the so-called reduced dimensionality method,[18] in which the numerical differentiation of analytical Hessians is performed only along selected normal modes (for instance, those providing the most intense IR bands at the harmonic level or those comprised in a specified frequency range). Note that this is not equivalent to consider only diagonal anharmonicity, since most couplings are retained in the final result.[61] For purposes of illustration, we analyze the vibrational bands of ferrocene in the 1400−3300 cm^{-1} region computing analytical Hessians at the B3LYP/II level for positive and negative displacements only along normal modes ranging from 40 to 57). Although the computational time is reduced to less than one-third of that needed for a full anharmonic treatment, the frequencies computed for the last two vibrations of ferrocene (1431 and 3121 cm^{-1}) are very close to those issuing from the complete calculation (1433 and 3120 cm^{-1}). This result points once again the effectiveness of reduced dimensionality models for the analysis of specific spectral regions.

4. CONCLUSION

Methods rooted in density functional theory have been employed to define a first benchmark for infrared (IR) spectroscopy at the anharmonic level for metallocene derivatives (Fe, Ru, and Os). All the calculations have been performed for the eclipsed conformation (D_{5h}), since many experimental and theoretical studies have revealed that this is the most stable one in the gas phase.

Full geometry optimizations showed substantial agreement with experimental data, for any combination of functionals and basis sets. Concerning ferrocene, the best agreement for Fe-Cp distances been reached at the CAM−B3LYP level, but also B3PW91 results can be considered fully satisfactory; in the case of ruthenocene, the B3PW91 functional and the LANL2DZ +pol basis set proved to be the best combination for the calculation of the Ru−C distance; osmocene follows the same trend as ruthenocene. The PBE0 functional underestimates the M−C distances for all three complexes. Finally, the computed equilibrium C−H bond lengths are, as expected, shorter than those provided by X-ray diffraction.

Vibrational frequencies have been calculated at the harmonic and anharmonic level, and compared to both experimental and theoretical data available in the literature. The results show that the addition of anharmonic terms is necessary to reach quantitative agreement with observed data for the three metallocenes. In contrast to the other functionals, BP86 shows a better agreement at the harmonic than at the anharmonic level, because of error compensation effects.

The calculated M−Cp vibrational frequencies of ferrocene at the anharmonic level show a good agreement with the experimental benchmark when one uses the PBE0 or B3PW91 functionals and an extended basis set. Furthermore, the computed ligand vibrations with B3LYP and B3PW91 functionals show very good agreement with experimental data. The entire $FeCp_2$ spectrum has been computed and the addition of both mechanical and electrical anharmonic corrections has led to a satisfactory agreement with experiment. The calculations also provide information in the region at ~1700 cm^{-1} (overtones), which are

dx.doi.org/10.1021/ct5006246 | J. Chem. Theory Comput. XXXX, XXX, XXX−XXX

completely absent at the harmonic level. Comparison shows that a strong peak near 630 cm^{-1} is not predicted by calculations: its position suggests that it is produced by a C−D bending motion of monodeuterated ferrocene. One should remark that LYP correlation has proved to be unable to correctly reproduce the M−Cp vibrational frequencies, while the PW91 one has provided very good agreement. Investigations similar to those outlined in this article are being performed on larger metal complexes.

Finally, the anharmonic results do not seem to be very sensitive to the choice of the functional and basis set, producing almost constant corrections. This latter result suggests that the most important factor in such calculations is to obtain good accuracy at the harmonic level. An interesting possibility left for future studies would be to use new double hybrid functionals with more extended basis sets (e.g., B2PLYP/cc-pVTZ[18]) for improving the harmonic part of the force field, provided that they retain the remarkable accuracy delivered for organic molecules also for transition-metal complexes.

■ ASSOCIATED CONTENT

Ⓢ Supporting Information

Tables containing the relevant geometric parameters and the vibrations of ruthenocene and osmocene. MAE vs experiment of computed ligand harmonic and anharmonic infrared vibrations of all metallocenes. The optimized Cartesian coordinates of B3PW91/IV for ferrocene. This material is available free of charge via the Internet at http://pubs.acs.org.

■ AUTHOR INFORMATION

Corresponding Author

*E-mails: camille.latouche@sns.it.

Notes

The authors declare no competing financial interest.

■ ACKNOWLEDGMENTS

The research leading to these results has received funding from the European Union's Seventh Framework Programme (FP7/2007-2013) under grant agreement No. ERC-2012-AdG-320951-DREAMS. The authors gratefully thank Dr. M. Piccardo for fruitful discussions and the high-performance computer facilities of the DREAMS center (http://dreamshpc.sns.it) for providing computer resources. The support of the COST CMTS-Action CM1002 `COnvergent Distributed Environment for Computational Spectroscopy (CODECS)" is also acknowledged.

■ REFERENCES

(1) Long, N. J. *Metallocenes: An Introduction to Sandwich Complexes*, 1st Edition; Wiley−Blackwell; New York, 1998; pp 1−285.
(2) Astruc, D. *Organometallic Chemistry and Catalysis*; Springer: Berlin, Heidelberg, Germany; 2007; pp 1−429.
(3) Bodenheimer, J.; Loewenthal, E.; Low, W. The Raman Spectra of Ferrocene. *Chem. Phys. Lett.* **1969**, *3*, 715−716.
(4) Bodenheimer, J. The Raman Spectra of Ruthenocene. *Chem. Phys. Lett.* **1970**, *6*, 519−520.
(5) Lokshin, B. V.; Aleksanian, V. T.; Rusach, E. B. On the Vibrational Assignments of Ferrocene, Ruthenocene and Osmocene. *J. Organomet. Chem.* **1975**, *86*, 253−256.
(6) Kissin, Y. *Alkene Polymerization Reactions with Transition Metal Catalysts*, 1st Edition; Elsevier Science: Amsterdam, 2008; pp 1−495.
(7) Yamaguchi, Y.; Palmer, B. J.; Kutal, C.; Wakamatsu, T.; Yang, D. B. Ferrocenes as Anionic Photoinitiators. *Macromolecules* **1998**, *31*, 5155−5157.
(8) Topçu Sulak, M.; Gökdoğan, Ö.; Gülce, A.; Gülce, H. Amperometric Glucose Biosensor Based on Gold-Deposited Poly-vinylferrocene Film on Pt Electrode. *Biosens. Bioelectron.* **2006**, *21*, 1719−1726.
(9) Hartinger, C. G.; Metzler-Nolte, N.; Dyson, P. J. Challenges and Opportunities in the Development of Organometallic Anticancer Drugs. *Organometallics* **2012**, *31*, 5677−5685.
(10) Bohn, R. K.; Haaland, A. On the Molecular Structure of Ferrocene, $Fe(C_5H_5)_2$. *J. Organomet. Chem.* **1966**, *5*, 470−476.
(11) Haaland, A.; Nilsson, J. The Determination of Barriers to Internal Rotation by Means of Electron Diffraction. Ferrocene and Ruthenocene. *Acta Chem. Scand.* **1968**, *22*, 2653−2670.
(12) Haaland, A.; Lusztyk, J.; Novak, D. P.; Brunvoll, J.; Starowieyski, K. B. Molecular Structures of Dicyclopentadienylmagnesium and Dicyclopentadienylchromium by Gas-Phase Electron Diffraction. *J. Chem. Soc. Chem. Commun.* **1974**, 54−55.
(13) Coriani, S.; Haaland, A.; Helgaker, T.; Jørgensen, P. The Equilibrium Structure of Ferrocene. *ChemPhysChem* **2006**, *7*, 245−249.
(14) Mohammadi, N.; Ganesan, A.; Chantler, C. T.; Wang, F. Differentiation of Ferrocene D_{5d} and D_{5h} Conformers Using IR Spectroscopy. *J. Organomet. Chem.* **2012**, *713*, 51−59.
(15) Alecu, I. M.; Zheng, J.; Zhao, Y.; Truhlar, D. G. Computational Thermochemistry: Scale Factor Databases and Scale Factors for Vibrational Frequencies Obtained from Electronic Model Chemistries. *J. Chem. Theory Comput.* **2010**, *6*, 2872−2887.
(16) Sinha, P.; Boesch, S. E.; Gu, C.; Wheeler, R. A.; Wilson, A. K. Harmonic Vibrational Frequencies: Scaling Factors for HF, B3LYP, and MP2 Methods in Combination with Correlation Consistent Basis Sets. *J. Phys. Chem. A* **2004**, *108*, 9213−9217.
(17) Andersson, M. P.; Uvdal, P. New Scale Factors for Harmonic Vibrational Frequencies Using the B3LYP Density Functional Method with the Triple-Z Basis Set 6-311+G(d,p). *J. Phys. Chem. A* **2005**, *109*, 2937−2941.
(18) Barone, V.; Biczysko, M.; Bloino, J. Fully Anharmonic IR and Raman Spectra of Medium-Size Molecular Systems: Accuracy and Interpretation. *Phys. Chem. Chem. Phys.* **2014**, *16*, 1759−1787.
(19) Barone, V. Anharmonic Vibrational Properties by a Fully Automated Second-Order Perturbative Approach. *J. Chem. Phys.* **2005**, *122*, 14108.
(20) Bloino, J.; Barone, V. A Second-Order Perturbation Theory Route to Vibrational Averages and Transition Properties of Molecules: General Formulation and Application to Infrared and Vibrational Circular Dichroism Spectroscopies. *J. Chem. Phys.* **2012**, *136*, 124108.
(21) Fabian, J. TDDFT-Calculations of Vis/NIR Absorbing Compounds. *Dye Pigment.* **2010**, *84*, 36−53.
(22) Jacquemin, D.; Perpète, E. A.; Scuseria, G. E.; Ciofini, I.; Adamo, C. Extensive TD-DFT Investigation of the First Electronic Transition in Substituted Azobenzenes. *Chem. Phys. Lett.* **2008**, *465*, 226−229.
(23) Jacquemin, D.; Wathelet, V.; Perpète, E. A.; Adamo, C. Extensive TD-DFT Benchmark: Singlet-Excited States of Organic Molecules. *J. Chem. Theory Comput.* **2009**, *5*, 2420−2435.
(24) Caricato, M.; Trucks, G. W.; Frisch, M. J.; Wiberg, K. B. Electronic Transition Energies: A Study of the Performance of a Large Range of Single Reference Density Functional and Wave Function Methods on Valence and Rydberg States Compared to Experiment. *J. Chem. Theory Comput.* **2010**, *6*, 370−383.
(25) Huang, S.; Zhang, Q.; Shiota, Y.; Nakagawa, T.; Kuwabara, K.; Yoshizawa, K.; Adachi, C. Computational Prediction for Singlet- and Triplet-Transition Energies of Charge-Transfer Compounds. *J. Chem. Theory Comput.* **2013**, *9*, 3872−3877.
(26) Puzzarini, C.; Biczysko, M.; Barone, V. Accurate Harmonic/Anharmonic Vibrational Frequencies for Open-Shell Systems: Performances of the B3LYP/N07D Model for Semirigid Free Radicals Benchmarked by CCSD(T) Computations. *J. Chem. Theory Comput.* **2010**, *6*, 828−838.
(27) Biczysko, M.; Panek, P.; Scalmani, G.; Bloino, J.; Barone, V. Harmonic and Anharmonic Vibrational Frequency Calculations with the Double-Hybrid B2PLYP Method. *J. Chem. Theory Comput.* **2010**, *6*, 2115−2125.

(28) Bloino, J.; Biczysko, M.; Barone, V. General Perturbative Approach for Spectroscopy, Thermodynamics, and Kinetics: Methodological Background and Benchmark Studies. *J. Chem. Theory Comput.* **2012**, *8*, 1015−1036.
(29) Frisch, M. J.; Trucks, G. W.; Schlegel, H. B.; Scuseria, G. E.; Robb, M. A.; Cheeseman, J. R.; Scalmani, G.; Barone, V.; Mennucci, B.; Petersson, G. A.; Nakatsuji, H.; Caricato, M.; Li, X.; Hratchian, H. R.; Izmaylov, A. F.; Bloino, J.; Zheng, G.; Sonnenberg, J. L.; Hada, M.; Ehara, M.; Toyota, K.; Fukuda, R.; Hasegawa, J.; Ishida, M.; Nakajima, T.; Honda, Y.; Kitao, O.; Nakai, H.; Vreven, T.; Montgomery Jr. J. A. Peralta, J. R.; Ogliaro, F.; Bearpark, M.; Heyd, J. J.; Brothers, E.; Kudin, K. N.; Staroverov, V. N.; Kobayashi, R.; Normand, J.; Raghavachari, K.; Rendell, A.; Burant, J. C.; Iyengar, S. S.; Tomasi, J.; Cossi, M.; Rega, N.; Millam, J. M.; Klene, M.; Knox, J. E.; Cross, J. B.; Bakken, V.; Adamo, C.; Jaramillo, J.; Gomperts, R.; Stratmann, R. E.; Yazyev, O.; Austin, A. J.; Cammi, R.; Pomelli, C.; Ochterski, J. W.; Martin, R. L.; Morokuma, K.; Zakrzewski, V. G.; Voth, G. A.; Salvador, P.; Dannenberg, J. J.; Dapprich, S.; Daniels, A. D.; Farkas, O.; Foresman, J. B.; Ortiz, J. V; Cioslowski, J.; Fox, D. J. *Gaussian 09, Revision D01*; Gaussian: Wallingford, CT, 2009.
(30) Becke, A. D. Density-Functional Exchange-Energy Approximation with Correct Asymptotic Behavior. *Phys. Rev. A* **1988**, *38*, 3098−3100.
(31) Perdew, J. P. Density-Functional Approximation for the Correlation Energy of the Inhomogeneous Electron Gas. *Phys. Rev. B* **1986**, *33*, 8822−8824.
(32) Becke, A. D. Density-Functional Thermochemistry. III. The Role of Exact Exchange. *J. Chem. Phys.* **1993**, *98*, 5648−5652.
(33) Perdew, J. P.; Burke, K.; Wang, Y. Generalized Gradient Approximation for the Exchange-Correlation Hole of a Many-Electron System. *Phys. Rev. B* **1996**, *54*, 16533−16539.
(34) Stephens, P. J.; Devlin, F. J.; Chabalowski, C. F.; Frisch, M. J. Ab Initio Calculation of Vibrational Absorption and Circular Dichroism Spectra Using Density Functional Force Fields. *J. Phys. Chem.* **1994**, *98*, 11623−11627.
(35) Lee, C.; Yang, W.; Parr, R. G. Development of the Colle-Salvetti Correlation-Energy Formula into a Functional of the Electron Density. *Phys. Rev. B* **1988**, *37*, 785−789.
(36) Adamo, C.; Barone, V. Toward Reliable Density Functional Methods without Adjustable Parameters: The PBE0Model. *J. Chem. Phys.* **1999**, *110*, 6158−6169.
(37) Ernzerhof, M.; Scuseria, G. E. Assessment of the Perdew−Burke−Ernzerhof Exchange-Correlation Functional. *J. Chem. Phys.* **1999**, *110*, 5029−5036.
(38) Yanai, T.; Tew, D. P.; Handy, N. C. A New Hybrid Exchange-Correlation Functional Using the Coulomb-Attenuating Method (CAM-B3LYP). *Chem. Phys. Lett.* **2004**, *393*, 51−57.
(39) Hay, P. J.; Wadt, W. R. Ab Initio Effective Core Potentials for Molecular Calculations. Potentials for the Transition Metal Atoms Sc to Hg. *J. Chem. Phys.* **1985**, *82*, 270−283.
(40) Wadt, W. R.; Hay, P. J. Ab Initio Effective Core Potentials for Molecular Calculations. Potentials for Main Group Elements Na to Bi. *J. Chem. Phys.* **1985**, *82*, 284−298.
(41) Hay, P. J.; Wadt, W. R. Ab Initio Effective Core Potentials for Molecular Calculations. Potentials for K to Au Including the Outermost Core Orbitals. *J. Chem. Phys.* **1985**, *82*, 299−310.
(42) Weigend, F.; Ahlrichs, R. Balanced Basis Sets of Split Valence, Triple Zeta Valence and Quadruple Zeta Valence Quality for H to Rn: Design and Assessment of Accuracy. *Phys. Chem. Chem. Phys.* **2005**, *7*, 3297−3305.
(43) Bergner, A.; Dolg, M.; Küchle, W.; Stoll, H.; Preuß, H. Ab Initio Energy-Adjusted Pseudopotentials for Elements of Groups 13−17. *Mol. Phys.* **1993**, *80*, 1431−1441.
(44) Kaupp, M.; Schleyer, P. v. R.; Stoll, H.; Preuss, H. Pseudopotential Approaches to Ca, Sr, and Ba Hydrides. Why Are Some Alkaline Earth MX2 Compounds Bent? *J. Chem. Phys.* **1991**, *94*, 1360−1366.
(45) Dolg, M.; Stoll, H.; Preuss, H.; Pitzer, R. M. Relativistic and Correlation Effects for Element 105 (hahnium, Ha): A Comparative Study of M and MO (M = Nb, Ta, Ha) Using Energy-Adjusted Ab Initio Pseudopotentials. *J. Phys. Chem.* **1993**, *97*, 5852−5859.
(46) Krishnan, R.; Binkley, J. S.; Seeger, R.; Pople, J. A. Self-Consistent Molecular Orbital Methods. XX. A Basis Set for Correlated Wave Functions. *J. Chem. Phys.* **1980**, *72*, 650−654.
(47) McLean, A. D.; Chandler, G. S. Contracted Gaussian Basis Sets for Molecular Calculations. I. Second Row Atoms, Z =11−18. *J. Chem. Phys.* **1980**, 72.
(48) Blaudeau, J.-P.; McGrath, M. P.; Curtiss, L. A.; Radom, L. Extension of Gaussian-2 (G2) Theory to Molecules Containing Third-Row Atoms K and Ca. *J. Chem. Phys.* **1997**, *107*, 5016−5021.
(49) Curtiss, L. A.; McGrath, M. P.; Blaudeau, J.; Davis, N. E.; Binning, R. C.; Radom, L. Extension of Gaussian-2 Theory to Molecules Containing Third-Row Atoms Ga−Kr. *J. Chem. Phys.* **1995**, *103*, 6104−6113.
(50) Mitin, A. V.; Baker, J.; Pulay, P. An Improved 6-31G* Basis Set for First-Row Transition Metals. *J. Chem. Phys.* **2003**, *118*, 7775−7783.
(51) Rassolov, V. A.; Pople, J. A.; Ratner, M. A.; Windus, T. L. 6-31G* Basis Set for Atoms K through Zn. *J. Chem. Phys.* **1998**, *109*, 1223−1229.
(52) Francl, M. M.; Pietro, W. J.; Hehre, W. J.; Binkley, J. S.; Gordon, M. S.; DeFrees, D. J.; Pople, J. A. Self-Consistent Molecular Orbital Methods. XXIII. A Polarization-Type Basis Set for Second-Row Elements. *J. Chem. Phys.* **1982**, *77*, 3654−3665.
(53) Dill, J. D.; Pople, J. A. Self-Consistent Molecular Orbital Methods. XV. Extended Gaussian-Type Basis Sets for Lithium, Beryllium, and Boron. *J. Chem. Phys.* **1975**, *62*, 2921−2923.
(54) Hehre, W. J.; Ditchfield, R.; Pople, J. A. Self-Consistent Molecular Orbital Methods. XII. Further Extensions of Gaussian-Type Basis Sets for Use in Molecular Orbital Studies of Organic Molecules. *J. Chem. Phys.* **1972**, *56*, 2257−2261.
(55) SNSD, basis sets. http://compchem.sns.it/sites/default/files/download/gaussian/basis_sets/SNSD.gbs. 2013.
(56) Xu, Z.-F.; Xie, Y.; Feng, W.-L.; Schaefer, H. F. Systematic Investigation of Electronic and Molecular Structures for the First Transition Metal Series Metallocenes $M(C_5H_5)_2$ (M = V, Cr, Mn, Fe, Co, and Ni). *J. Phys. Chem. A* **2003**, *107*, 2716−2729.
(57) Bobyens, J. C. A.; Levendis, D. C.; Bruce, M.; Williams, M. Crystal Structure of Osmocene, $Os(\eta\text{-}C_5H_5)_2$. *J. Crystallogr. Spectrosc. Res.* **1986**, *16*, 519−524.
(58) Lippincott, E.; Nelson, R. The Vibrational Spectra and Structure of Ferrocene and Ruthenocene. *Spectrochim. Acta* **1958**, *10*, 307−329.
(59) Gryaznova, T. P.; Katsyuba, S. A.; Milyukov, V. A.; Sinyashin, O. G. DFT Study of Substitution Effect on the Geometry, IR Spectra, Spin State and Energetic Stability of the Ferrocenes and Their Pentaphospholyl Analogues. *J. Organomet. Chem.* **2010**, *695*, 2586−2595.
(60) Kimel'fel'd, Y.; Smirnova, E.; Aleksanyan, V. The Vibrational Spectra of Molecular Crystals of Ferrocene, Ruthenocene, Osmocene and Nickelocene. *J. Mol. Struct.* **1973**, *19*, 329−346.
(61) Barone, V.; Biczysko, M.; Bloino, J.; Borkowska-Panek, M.; Carnimeo, I.; Panek, P. Toward Anharmonic Computations of Vibrational Spectra for Large Molecular Systems. *Int. J. Quantum Chem.* **2012**, *112*, 2185−2200.